SYNCHRONIZATION OF ENERGY CAPTURE RECEIVERS FOR UWB APPLICATIONS

Cecilia Carbonelli and Umberto Mengali

Department of Information Engineering, University of Pisa
Via Caruso, 56100 Pisa
{cecilia.carbonelli@iet.unipi.it, umberto.mengali@iet.unipi.it}

ABSTRACT

The paper investigates simple timing recovery schemes for M-PPM non-coherent ultra-wideband receivers. Their performance is assessed by simulation over realistic multipath channels. The degradations due to timing errors are found to be marginal.

1. INTRODUCTION

Several timing algorithms for ultra-wideband (UWB) PAM correlation receivers have been proposed in the literature [1]-[2]-[3]. They exploit training sequences and are based on correlation operations. In the following we concentrate on noncoherent (energy capture) UWB receivers for M-ary pulse position modulation (M-PPM). The synchronization problem for M-PPM has been extensively investigated in connection with optical communications [5]-[6]-[7]. In optical systems the light intensity is varied in an on/off fashion and the pulse edges at the photo-detector output are exploited for timing recovery. In UWB systems, vice versa, the received pulses have no fixed shape. They result from the superposition of hundreds of echoes of the same excitation pulse (monocycle), arriving at the receiver with different attenuations and delays. As a consequence, their shape is highly dependent on the physical environment and the receiver location.

This paper investigates simple feedback timing recovery schemes wherein the error signal is derived from energy measurements. No information is required about the transmitted data (blind operation). Simulations show that the timing accuracy is quite satisfactory and the synchronization errors have a marginal impact on the bit error rate.

The advantage of blind timing recovery is that, while in [1]-[2]-[3]-[4] the timing estimates must be periodically updated to cope with the channel variations, in our case the channel variations are continuously tracked with no penalty in information rate. Also, blind synchronization greatly simplifies the channel access protocol and provides quick recovery from link failures.

The rest of the paper is organized as follows. In the next Section we describe the signal model and the receiver structure. Section 3 deals with the synchronization scheme for 2-PPM while Section 4 extends the results to M-ary modulation. Conclusions are drawn in Section 5.

This work was supported by the Italian Ministry of Education in the framework of the project PRIMO, FIRB 2001

2. SIGNAL MODEL

With M-PPM modulation the signaling interval of duration T is divided into M equal slots and a monocycle is transmitted at the beginning of one slot. After travelling through the channel and passing through a rectangular low-pass filter of bandwidth B, the received waveform takes the form

$$r(t) = \sum_{k=-\infty}^{\infty} h(t - kT - a_k T/M - \tau) + n(t) \qquad (1)$$

In this formula $h(t)$ is the channel response to a monocycle. We assume it totally unknown except for its duration which is limited within $0 \le t \le T_{mds}$, where T_{mds} is the channel's maximum delay spread. The a_k are M-ary independent and identically distributed data symbols taken from the alphabet $A = \{0, 1, ...M-1\}$. Also, $n(t)$ is the thermal noise, which is modelled as a white Gaussian process with power spectral density $N_0/2$ in the interval $-B \le f \le B$. Finally, τ represents the time offset between the transmit and receive clocks.

Notice that (1) implies a static channel since $h(t)$ has a fixed shape. Although this limitation might be relaxed by letting $h(t)$ vary from symbol to symbol, in the following we stick to (1) for notational simplicity. Observe that no time-hopping is performed to enable multiple access to the transmission medium. Channel sharing must be accomplished in a time-division fashion.

It has been shown in [8] that if no channel information is exploited for detection purposes, application of the generalized maximum ratio test leads to an energy capture receiver and the optimum decision rule consists of comparing the signal energies received in the M slots of a symbol interval and deciding that the transmitted pulse is located in the slot with maximum energy. In other terms, the estimate of a_k is obtained as

$$\hat{a}_k = \arg \max_{m \in [0, M-1]} z_{Mk+m} \qquad (2)$$

where

$$z_{Mk+m} := \int_{t_{Mk+m}}^{t_{Mk+m}+\Delta} r^2(t) dt \qquad (3)$$

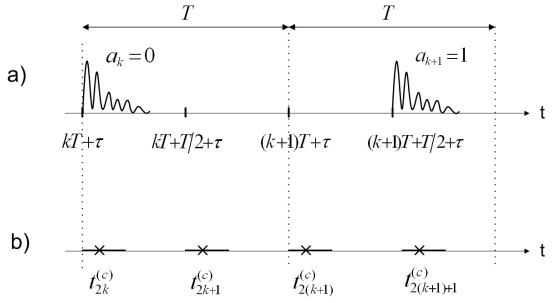

Figure 1: Illustrating the output of the squarer in Fig.1

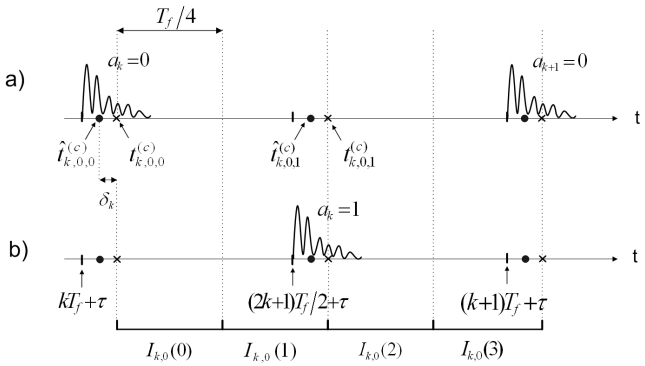

Figure 2: Illustrating the integrals $I_k(l)$

$t_{Mk+m} := (Mk+m)T/M$ and the choice of the integration interval Δ depends on the channel's delay profile [8].

3. SYNCHRONIZATION FOR 2-PPM

As indicated in (2)-(3), the computation of the decision statistics z_{Mk+m} requires knowledge of the slot starting times. This information must be provided by a synchronizer. In this section we address the synchronization problem for 2-PPM. To ease the discussion we assume that the noise is negligible but its effects are taken into account in the simulations.

Figure 1a illustrates the waveform $r^2(t)$. The signal model (1) is assumed, with the slots of the k-th symbol starting at the epochs $kT+\tau$ and $kT+T/2+\tau$. It is seen that in the k-th symbol interval the channel response appears in the first slot ($a_k=0$) while, in the next interval, it comes out in the second slot ($a_{k+1}=1$). The integration intervals (each of size Δ) are shown in Fig. 1b in solid segments, with crosses indicating the *centers* $t_{2k+m}^{(c)}$ of the channel responses. For an $h(t)$ originating at $t=\bar{t}$, the center $\bar{t}^{(c)}$ is implicitly defined as

$$\int_{\bar{t}}^{\bar{t}^{(c)}} h^2(t-\bar{t})dt = \int_{\bar{t}^{(c)}}^{\infty} h^2(t-\bar{t})dt \qquad (4)$$

or equivalently, letting $\delta_{left} := \bar{t}^{(c)} - \bar{t}$,

$$\int_0^{\delta_{left}} h^2(t)dt = \int_{\delta_{left}}^{\infty} h^2(t)dt \qquad (5)$$

In essence, δ_{left} is the *mid-energy* point of $h(t)$. It follows that the channel response centers (CRCs) may be expressed as $t_{2k+m}^{(c)} = kT+mT/2+\tau+\delta_{left}$ $(m=0,1)$.

The relevance of the CRCs stems from the fact that, if they were known, the integration intervals in (3) might be computed as $-\delta_{left} \le t - t_{2k+m}^{(c)} \le \Delta - \delta_{left}$ or, more compactly,

$$-\delta_{left} \le t - t_{2k+m}^{(c)} \le \delta_{right} \qquad (6)$$

with $\delta_{right} := \Delta - \delta_{left}$. It is clear from (5) that parameters δ_{left} and δ_{right} cannot be computed as they depend on the actual shape of $h(t)$ which is unknown. Thus, we approximate them with fixed quantities, Δ_{left} and Δ_{right}.

For a given channel model the best choice of Δ_{left} and Δ_{right} can be established by simulation assuming perfect knowledge of the CRCs. For example with a CM3 channel ([9]) and $\Delta = 40$ ns we have found that taking Δ_{left}=20 ns entails a degradation of 0.1 dB in terms signal-to-noise ratio at BER$= 10^{-3}$ with respect to the ideal receiver with perfect knowledge of δ_{left} and δ_{right}. The corresponding degradation with a CM2 channel ([9]) is about 0.2 dB for $\Delta = 25$ ns and Δ_{left}=10 ns. Although the simulations were run with a symbol period $T = 300$ ns and a monocycle shaped as the second derivative of a Gaussian function of duration 1 ns, the results hold true in general provided that the pulse duration is much shorter than the channel delay spread and there is no inter-slot interference.

At this stage we address the estimation of the CRCs. Figure 2 depicts a symbol-long stretch of $r^2(t)$ along with the CRCs (cross marks). Two possible channel responses are shown, corresponding to either $a_k=0$ or $a_k=1$. To begin, we denote by $\hat{t}_{2k}^{(c)}$ and $\hat{t}_{2k+1}^{(c)}$ tentative values of $t_{2k}^{(c)}$ and $t_{2k+1}^{(c)}$ (with $\hat{t}_{2k+1}^{(c)} = \hat{t}_{2k}^{(c)} + T/2$) and we look for the unknown shift $\delta_k := t_{2k}^{(c)} - \hat{t}_{2k}^{(c)} = t_{2k+1}^{(c)} - \hat{t}_{2k+1}^{(c)}$. As is now explained, information on this quantity is obtained from the integrals

$$I_k(\ell) := \int_{\hat{t}_{2k}^{(c)}+\ell T/4}^{\hat{t}_{2k}^{(c)}+(\ell+1)T/4} r^2(t)dt \qquad \ell = 0,1,2,3 \qquad (7)$$

through the error signal

$$e(k) = [I_k(0)+I_k(2)] - [I_k(1)+I_k(3)] \qquad (8)$$

Clearly, $e(k)$ is a random variable, not just a deterministic function of δ_k. Still, assuming a channel response shorter than $T/4$, from Fig. 2 we realize that the average of $e(k)$ is zero for $\delta_k = 0$ and varies periodically with δ_k with period $T/2$. Figure 3 illustrates the conditional expectation $S(\delta) := E\{e(k)\,|\,\delta_k = \delta\}$ (also known as *S-curve*) as obtained by simulation with a CM3 channel. The very form of the S-

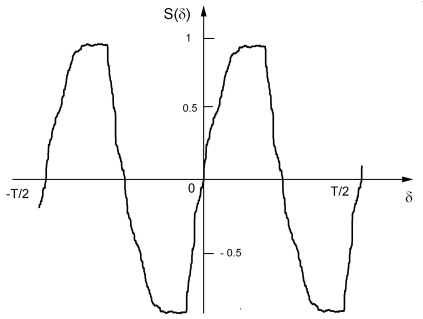

Figure 3: S-curve for 2-PPM and CM3 channel

curve suggests computing $\hat{t}_{2k}^{(c)}$ recursively as

$$\hat{t}_{2(k+1)}^{(c)} = \hat{t}_{2k}^{(c)} + T + \gamma e(k) \tag{9}$$

where γ is a step-size parameter and k ticks at symbol rate. The rationale behind this formula is grasped by approximating $e(k)$ with its expectation $S(\delta_k)$ and subtracting (9) from $t_{2(k+1)}^{(c)} = t_{2k}^{(c)} + T$. As a result we get

$$\delta_{k+1} = \delta_k - \gamma S(\delta_k) \tag{10}$$

The steady-state solutions ($\delta_k = \delta_\infty$=constant) of (10) are such that $S(\delta_\infty) = 0$ and the derivative of $S'(\delta_\infty)$ is positive [10]. From Fig. 3 we see that this occurs [1] for either $\delta_\infty = 0$ or $\delta_\infty = -T/2$. The first case corresponds to $\hat{t}_{2k}^{(c)} \cong t_{2k}^{(c)}$, which is the desirable occurrence, while the other corresponds to $\hat{t}_{2k}^{(c)} \cong t_{2k}^{(c)} + T/2 = t_{2k+1}^{(c)}$, meaning that the estimated CRCs are shifted by half a symbol compared to the true CRCs. In the latter case the detector decisions would be totally unreliable. For CM3 channel and with $\gamma = 0.25$ the timing errors reduce to very small values in about 2000 symbols. Increasing γ shortens the acquisition time at the cost of increased error fluctuations in the steady state.

From the above discussion it appears that some means must be devised to distinguish a *true lock* ($\hat{t}_{2k}^{(c)} \cong t_{2k}^{(c)}$) from a *false lock* ($\hat{t}_{2k}^{(c)} \cong t_{2(k-1)+1}^{(c)}$). This problem is now addressed assuming that a steady-state condition has been achieved so that the estimated CRCs are either aligned with the true CRCs (in-lock) or are shifted by $T/2$ (out-of-lock). The reasoning hinges on the decision statistics in (3) which, within the approximations made so far, may be rewritten as

$$z_{2k+m} = \int_{\hat{t}_{2k+m}^{(c)} - \Delta_{left}}^{\hat{t}_{2k+m}^{(c)} + \Delta_{right}} r^2(t)dt \tag{11}$$

[1] It is sufficient to limit ourselves to the interval $-T/2 \le \delta_\infty < T/2$ since a non-data-aided synchronizer can only recover timing within multiples of the symbol period.

The statistics of the random variable $w_{2k} := z_{2k} + z_{2k+1}$ depend on whether the synchronizer is in-lock or out-of-lock so that we can take advantage of this fact to distinguish between the two operating conditions. For the sake of argument suppose that the noise is negligible so that the integral in (11) is either a positive constant A or 0, depending on whether a channel response around $\hat{t}_{2k+m}^{(c)}$ is present or not. In the in-lock condition the integration intervals for z_{2k} and z_{2k+1} belong to the same symbol interval so that only two alternatives are possible: either the channel response is in the first slot ($z_{2k} = A$, $z_{2k+1} = 0$) or it is in the second slot ($z_{2k} = 0$, $z_{2k+1} = A$). In both cases w_{2k} equals A. In the out-of-lock condition, vice versa, the integration intervals for z_{2k} and z_{2k+1} belong to different symbol intervals so that four equiprobable events may occur: ($z_{2k} = 0$, $z_{2k+1} = 0$), ($z_{2k} = 0$, $z_{2k+1} = A$), ($z_{2k} = A$, $z_{2k+1} = 0$), ($z_{2k} = A$, $z_{2k+1} = A$). Correspondingly, we have $w_{2k} = A$ with probability 1/2, $w_{2k} = 0$ with probability 1/4 and $w_{2k} = 2A$ with probability 1/4. In conclusion, w_{2k} has still the same mean A as before but its variance is nonzero. In the presence of noise the picture is more complicated but the conclusion is the same: the variance of w_{2k} achieves a minimum in the in-lock condition.

Based on these considerations the in-lock/out-of-lock alternative can be resolved with a simple test. Taking the decision statistics over N symbols we compare the sample variance of $z_{2k} + z_{2k+1}$ with the sample variance of $z_{2k+1} + z_{2(k+1)}$ and we decide that the synchronizer is in lock if the former is smaller than the latter. In formulas

$$\frac{1}{N}\sum_{k=0}^{N-1}(z_{2k} + z_{2k+1} - \bar{w})^2 \underset{\text{out-of-lock}}{\overset{\text{in-lock}}{\lessgtr}} \frac{1}{N}\sum_{k=0}^{N-1}(z_{2k+1} + z_{2(k+1)} - \bar{w})^2 \tag{12}$$

where $\bar{w}$ is the sample mean of either $z_{2k} + z_{2k+1}$ or $z_{2k+1} + z_{2(k+1)}$.

4. EXTENSION TO M-PPM

The synchronization scheme discussed above is now extended to higher-order modulations. With M-ary modulation there are M distinct CRCs in a symbol interval, one in each slot. We call $t_{Mk+m}^{(c)}$ and $\hat{t}_{Mk+m}^{(c)}$ the true and estimated CRCs in the m-the slot of the k-th interval. The decision statistics are now

$$z_{Mk+m} = \int_{\hat{t}_{Mk+m}^{(c)} - \Delta_{left}}^{\hat{t}_{Mk+m}^{(c)} + \Delta_{right}} r^2(t)dt \qquad m = 0, 1, \ldots M-1 \tag{13}$$

while the error signal is a function of the integrals

$$I_k(\ell) := \int_{\hat{t}_{Mk}^{(c)} + \ell T/(2M)}^{\hat{t}_{Mk}^{(c)} + (\ell+1)T/(2M)} r^2(t)dt \qquad \ell = 0, 1, 2, \ldots 2M-1 \tag{14}$$

and is expressed as

$$e(k) = \sum_{\ell=0}^{M-1} [I_k(2\ell) - I_k(2\ell+1)] \tag{15}$$

Finally, the updating of the CRC estimates is performed as

$$\hat{t}^{(c)}_{M(k+1)} = \hat{t}^{(c)}_{Mk} + T + \gamma e(k) \tag{16}$$

with k ticking at symbol rate. The error signal gives unbiased measurements of the timing error provided that the channel response is shorter than $T/(2M)$. As the channel response is independent of the number of modulation levels, this implies that the symbol period must be increased as M increases.

In the simulations we set $T = 300$ ns with 2-PPM, $T = 600$ ns with 4-PPM and $T = 1200$ ns with 8-PPM. These values are compatible with the condition $T_{mds} < T/M$ since the maximum delay spread is about 60 ns with CM3 and even smaller with CM1 and CM2. Furthermore, the S-curves for 4-PPM and 8-PPM with a CM3 channel are periodic with period $T/4$ and $T/8$, respectively, and exhibit either four or eight zero-crossings with positive slope in a symbol period. Only the zero-crossing in the origin corresponds to a correct operating condition, meaning that true and estimated CRCs are aligned. In the other cases the misalignment is a multiple of a slot period. Again, an in-lock detector is needed. To this end the same idea adopted previously may be followed. It consists of computing the sample variance of $\sum_{l=0}^{M-1} z_{Mk+m+l}$ $(m = 0, 1, ..., M-1)$ and looking for its minimum as a function of m. The corresponding value of m, say $\hat{m}$, gives the in-lock position. In formulas

$$\hat{m} = \arg\min_m \frac{1}{N} \sum_{k=0}^{N-1} \left(\sum_{l=0}^{M-1} z_{Mk+m+l} - \bar{w} \right)^2 \tag{17}$$

where $\bar{w}$ is the sample mean of $\sum_{l=0}^{M-1} z_{Mk+m+l}$. Some attention should be paid to the subscript of z_{Mk+m+l} for m and ℓ varying in the interval $[0, M-1]$. Calling k' the integer part of $(m+\ell)/M$ and setting $m' := (m+\ell) \bmod M$, we may write

$$z_{Mk+m+l} = z_{M(k+k')+m'} \tag{18}$$

indicating that z_{Mk+m+l} is the decision statistic from the m'-th slot of the $(k+k')$-th symbol interval. Fig. 4 shows simulations illustrating the effects of synchronization errors on the BER performance. Black dots correspond to perfect knowledge of the CRCs (ideal synch) while white dots are computed taking the CRCs from the synchronizer (practical synch). It is seen that the the results are virtually the same.

5. CONCLUSIONS

We have addressed the synchronization issue for UWB noncoherent receivers and we have proposed a feedback timing recovery loop wherein the error signal is computed from energy measurements. It has been shown that the loop may get stuck in false locks, depending on the initial conditions at the receiver's start up. A simple test has been indicated to establish the in-lock condition. The BER degradations due to timing errors have been found marginal.

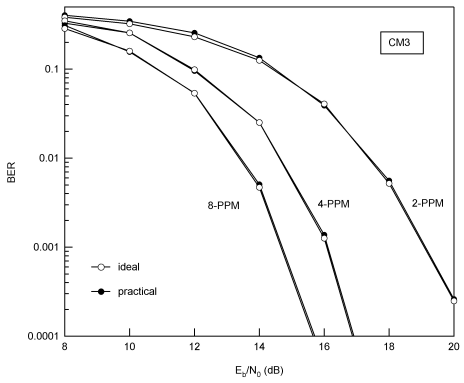

Figure 4: BER curves illustrating the impact of synchronization errors

REFERENCES

[1] C. Carbonelli and U. Mengali, "Timing recovery for UWB signals," in *Proceedings GLOBECOM'04*, (Dallas, TX), December 2004.

[2] Z. Tian and G. Giannakis, "Data-aided ML timing acquisition in ultra-wideband radios," in *Proceedings of IEEE Symposium on Ultra-Wideband Systems and Technologies*, (Reston, VA), November 2003.

[3] Z. Tian and G. Giannakis, "A GLRT approach to data-aided timing acquisition in UWB radios - Part I : Algorithms," *IEEE Transactions on Wireless Communications (to appear)*.

[4] A. Rabbachin and I. Oppermann, "Synchronization analysis for UWB systems with a low-complexity energy collection receiver," in *Proceedings of IEEE Symposium on Ultra-Wideband Systems and Technologies*, (Kyoto, Japan), May 2004.

[5] U. Mengali, "Timing recovery in optical data transmission," *Opt. Quant. Electon.*, vol. 9, pp. 383–391, 1977.

[6] R. N. Gagliardi, "Synchronization using pulse edge tracking in optical pulse position modulated communication systems," *IEEE Transactions on Communications*, vol. COM-22, pp. 1693–1702, October 1974.

[7] C. N. Georghiades, "Maximum likelihood symbol synchronization for the direct detection optical on-off-keying channel," *IEEE Transactions on Communications*, vol. COM-35, pp. 626–631, June 1987.

[8] C. Carbonelli and U. Mengali, "Low complexity synchronization for noncoherent UWB receivers," accepted for presentation at *VTC05*, (Stockholm, Sweden), June 2005.

[9] IEEE P802.15 Working Group for Wireless Personal Area Network, "Channel model subcommittee report final," tech. rep., December 2002.

[10] U. Mengali and A. N. D'Andrea, *Synchronization Techniques for Digital Receivers*. New York: Plenum Press, 1997.